

Energy harvesting in a beam system with an additional moving mass

Andrzej Rysak, Michael Scheffler, Joachim Gier, Marek Borowiec,
Grzegorz Litak

Abstract: We examine energy harvesting by using the composite laminate beam with a moving mass subjected to kinematic harmonic excitation. The moving tip mass applied to the system is softening in the spring characteristic of the beam. Simultaneously, we observed also additional damping and other non-linear effects of friction caused by this mass. The experiments have been performed on the beam excited kinematically by a shaker, while measurements were made by the scanning laser vibrometer. In the limit of small excitation level we applied the modal analysis. The selected modal vibration were illustrated by time series.

1. Introduction

The influence of additional degree of freedom usually introduces additional frequency response. This effect has been already used in energy harvesting to broaden the region of frequency response. Nana and Wofo [1] suggested the use of an array of two or more harvesters to increase the power delivered into the load. Shahruz [2] analyzed a set of parallel single degree of freedom harvesters tuned at slightly different resonant frequencies, whereas Erturk et al. [3] considered a harvester as a serial set of two L-shaped beams. Recently, Litak et al. [4] and Kucab et al. [5] studied two coupled magnetopiezoelectric oscillators with mistuning. They reported the effects of nonlinearities on the synchronization of the oscillators and consequently on the power output.

In our case the moving mass (Fig. 1b) would cause impact and friction phenomena. In general, the nonlinear effects improve the effectiveness of energy harvesting systems by broadening frequency intervals in the resonance region [4,6]. Such devices of energy harvesting contain mechanical resonators and additional energy transducers for transforming ambient mechanical energy into the electric form. Following this concept Gu and Livermore

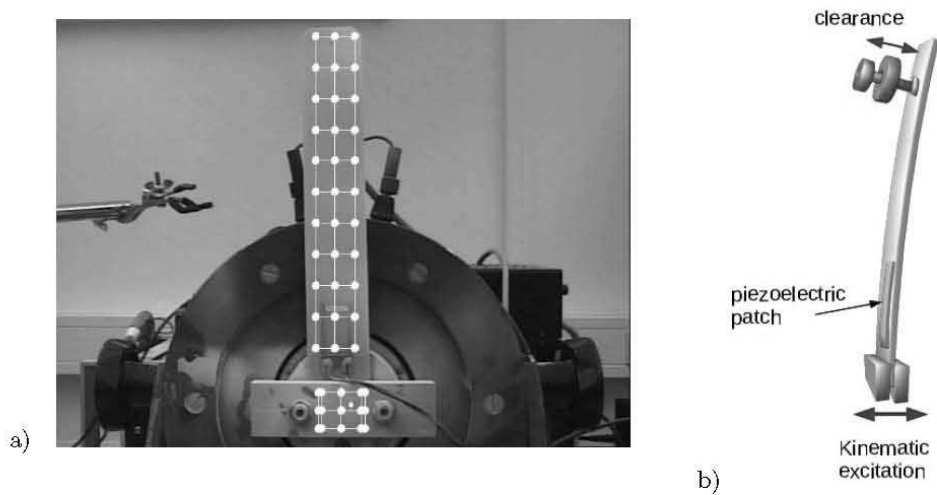


Figure 1. Photo of the experimental stand (a), and schematic plot of the beam with moving element (b).

[7] presented experimental results of models of energy harvesting devices in which a low frequency resonator impacts a high frequency harvesting resonator. The experiments with impacts demonstrate that the efficiency of the electrical power transfers can significantly be improved [8-10].

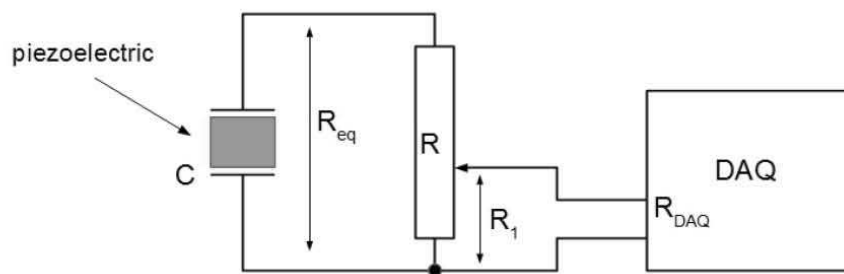


Figure 2. Electrical circuit set with the electro-motive force on the piezoceramic element; electric resistors with the data acquisition system DAQ and voltage divider.

In the present experimental model, the influence of a moving mass on the efficiency of the piezoelectric transducers is investigated. This mass can cause the additional dissipation via a friction phenomena. Note that interrupted contact of the moving mass with the cantilever (Fig. 1b) does change the effective spring characteristics of the vibrating beam which increases the resonant frequency.

2. Experimental model

In the experiment we investigated the piezoelectric patch using d_{31} -effect. During the beam vibration, the electric power generated by the piezoelectric loaded the corresponding resistors. The electrical output was measured by means of data acquisition set (DAQ) (see Fig. 2) as:

$$U_{DAQ} = U_{out} \frac{R_1}{R}, \quad (1)$$

where the ratio R_1/R is the voltage divider presented in Fig. 2, applied to avoid exceeding the measurement voltage range. In the experiments we used a piezoceramic patch layer attached to the beam. The diagram of the beam used in the experiments together with the labels of dimensions and corresponding sizes is presented in Fig. 3.

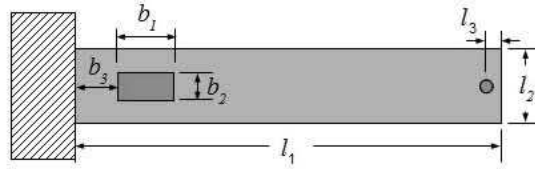


Figure 3. Diagram of the beam with MFC (Macro Fiber Composite). Marked dimensions are given in table 1.

Table 1. Parameters of the mechanical resonator and electrical circuit.

Symbol and value	Description
$l_1 = 198$ mm	beam length
$l_2 = 35$ mm	beam width
$h = 2.2$ mm	beam thickness
$l_3 = 10$ mm	position of the mass
$b_1 = 37$ mm	the length of the piezoelectric layer
28 mm	active layer length
$b_2 = 18$ mm	the width of the piezoelectric layer
14 mm	active layer width
$b_3 = 12$ mm	position of the piezoelectric layer
$C = 29.5$ nF	capacity of the piezoceramic layer

To measure the corresponding velocities of the beam and frame we used the scanning laser vibrometer. For a low level of excitations, we performed the standard modal analysis to find the characteristic mode shapes and its eigen-frequencies (see Fig. 4).

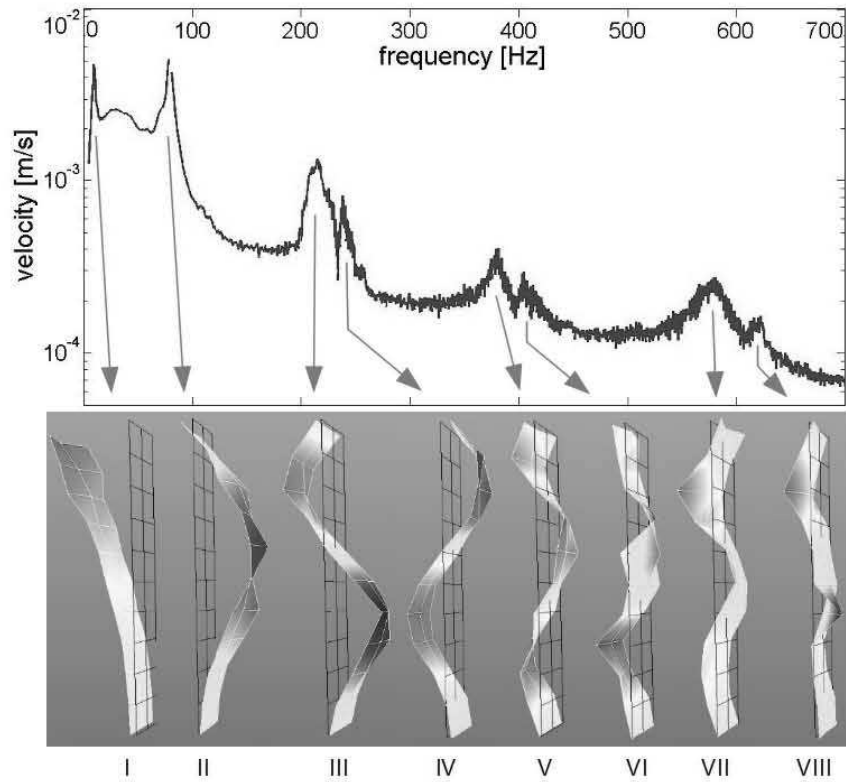


Figure 4. Modal analysis of the vibrating beam. The corresponding mod shapes are plotted below and numbered with the roman numbers.

3. Analysis of experimental results

After the scanning measurements (see the grid pints depicted on the excited beam and reference frame in Fig. 1a), we performed the modal analysis.

Modal analysis is focused on movement behavior of a mechanical structure in dependence of space and time. Indicators of this movement are: eigen-values, consisting of eigen-frequencies, modal dampings, and eigen-vectors. The eigenvectors (deflection shapes of the structure) are closely related to the eigen-frequencies. The shapes are only determined by the inner composition of structure and its parameters. In the opposite there are existing operational deflection shapes induced by a specific excitation due to the action of the structure. In this case, following vibrational behavior is determined as well as by the composition of structure as excitation. Excitation means both time function shape as their location.

The 2nd order set of linearized equations of motion for a discretized mechanical system

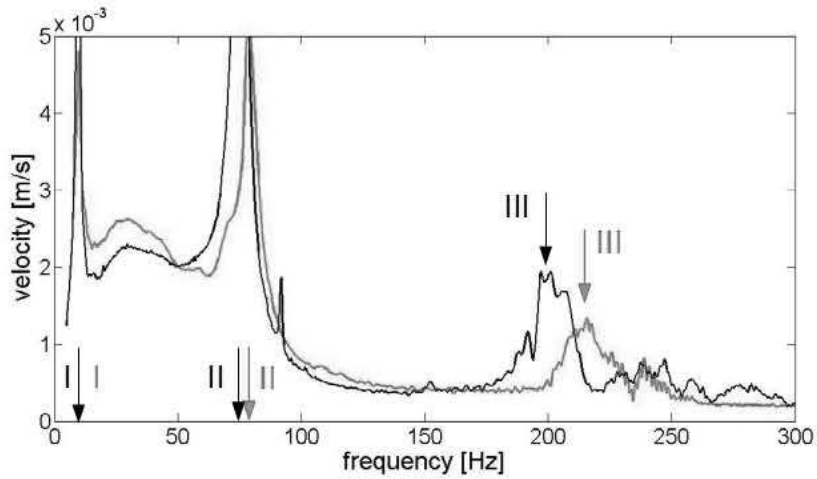


Figure 5. Magnification of the first three vibration modes for the system with moving (violet color) and fixed (black color) masses.

Table 2. The ratio of the standard deviation of the output voltage (measured on the piezoceramic part) to the standard deviation of the reference signal.

Vibration Mod	Fixed mass	Mass with clearance
I	1.0827	0.4353
II	1.5601	1.1210
III	1.5459	1.4612

of N DOF (corresponding to the number of measured points)

$$\mathbf{M}\ddot{\mathbf{y}} + \mathbf{K}\dot{\mathbf{y}} + \mathbf{C}\mathbf{y} = \mathbf{f}(t), \quad (2)$$

where $\mathbf{y}(t)$ and $\mathbf{f}(t)$ are the vectors of generalized coordinates and generalized force, while \mathbf{M} , \mathbf{K} and \mathbf{C} , are mass, damping, and stiffness matrices, respectively. Note that the modal parameters (\mathbf{M} , \mathbf{K} and \mathbf{C}) are unknown and are to be found experimentally, together with corresponding node shapes, as the eigenvectors.

The modal analysis for the beam with moving mass results in the frequency domain together with the selected modal shape pictures are presented in Fig. 4. The modal analysis is designed for the linear systems. In our studies we followed it for a fairly low excitation level.

However it is possible to see that the mode shapes do not represent the smooth surfaces which was expected for the system effected by friction and impacts. Similarly, the line

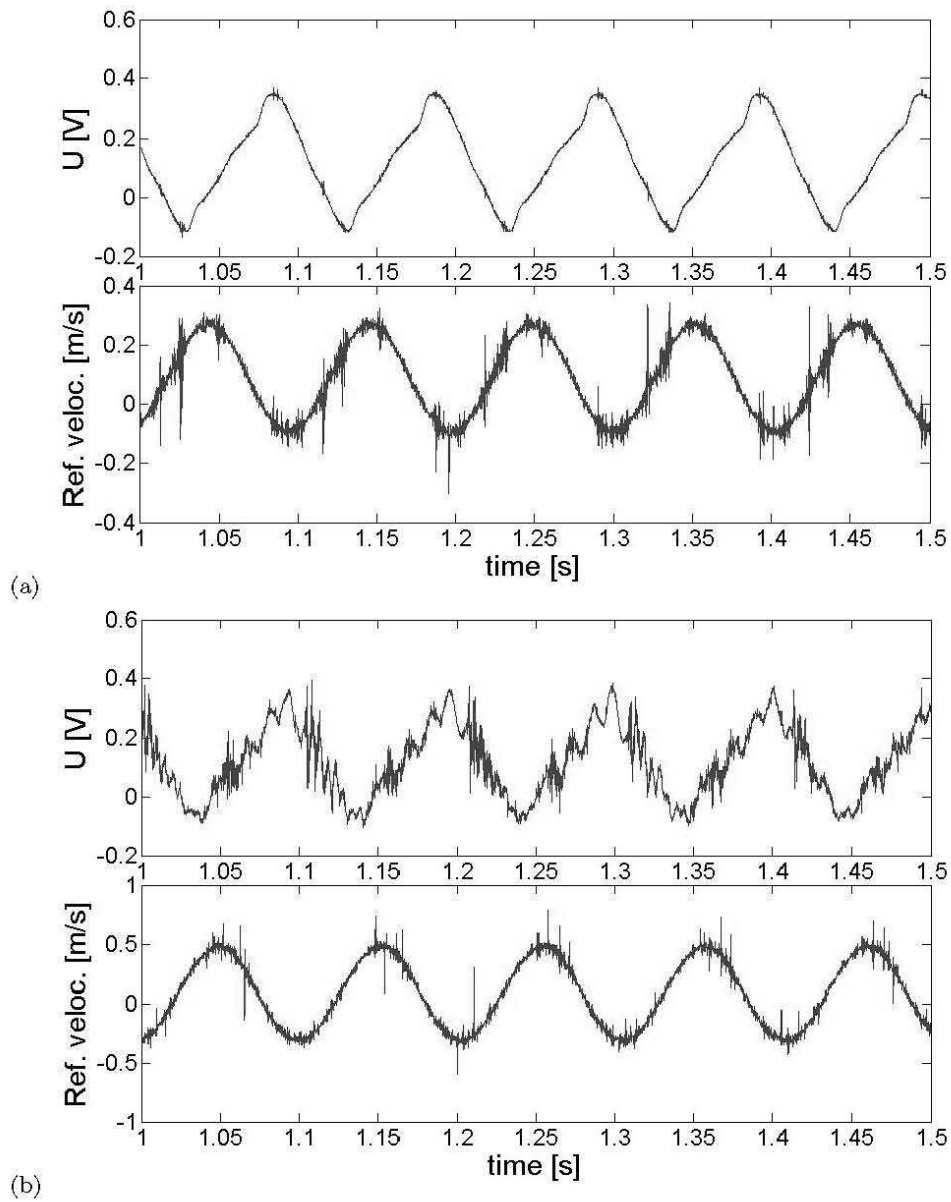


Figure 6. Time series for the first mode of the beam with fixed tip mass at the frequency $f = 9.96$ Hz (a) and moving mass at $f = 9.96$ Hz (b). Note that above there is the voltage output while below we plot the measured shaker velocity

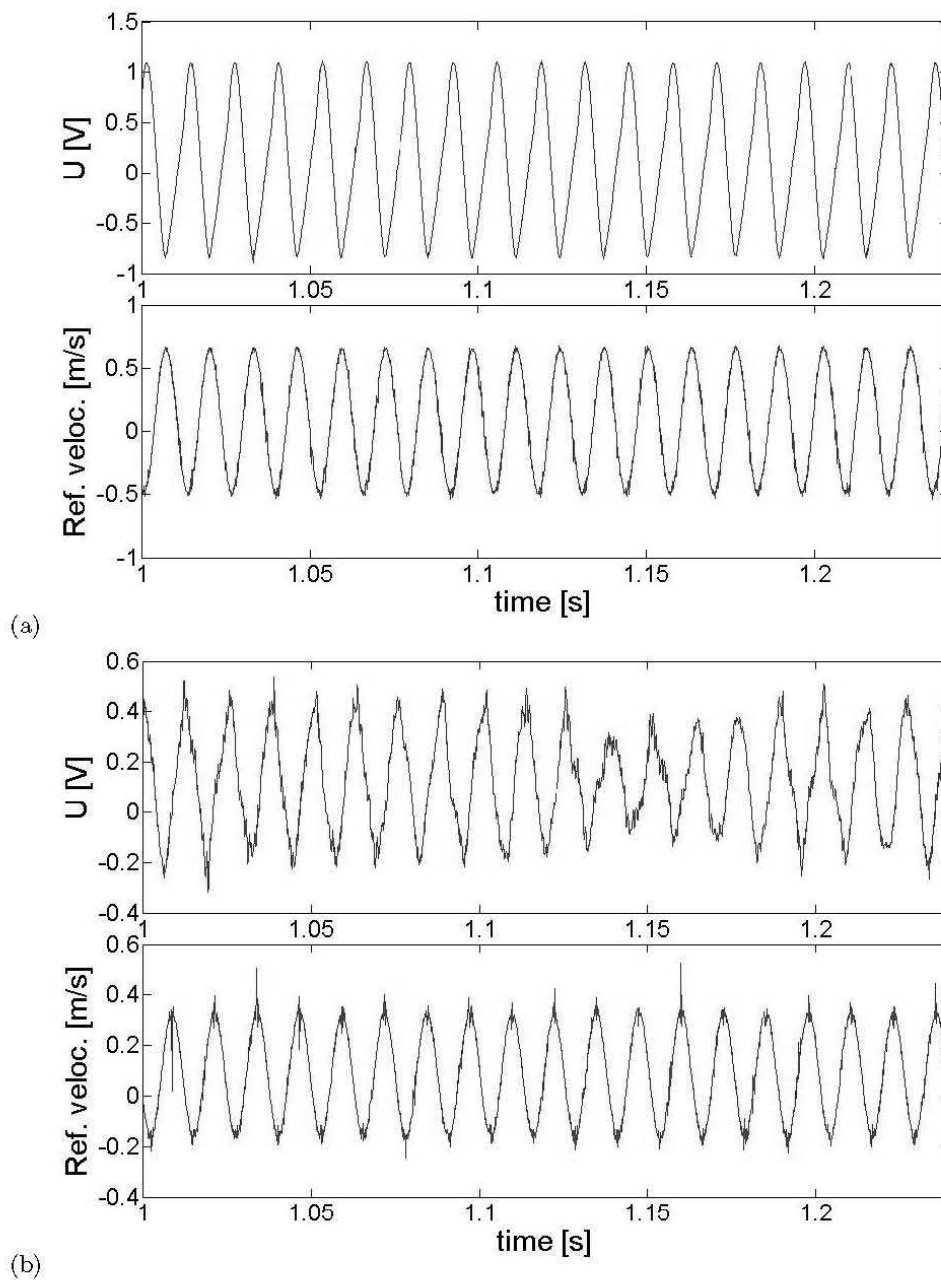
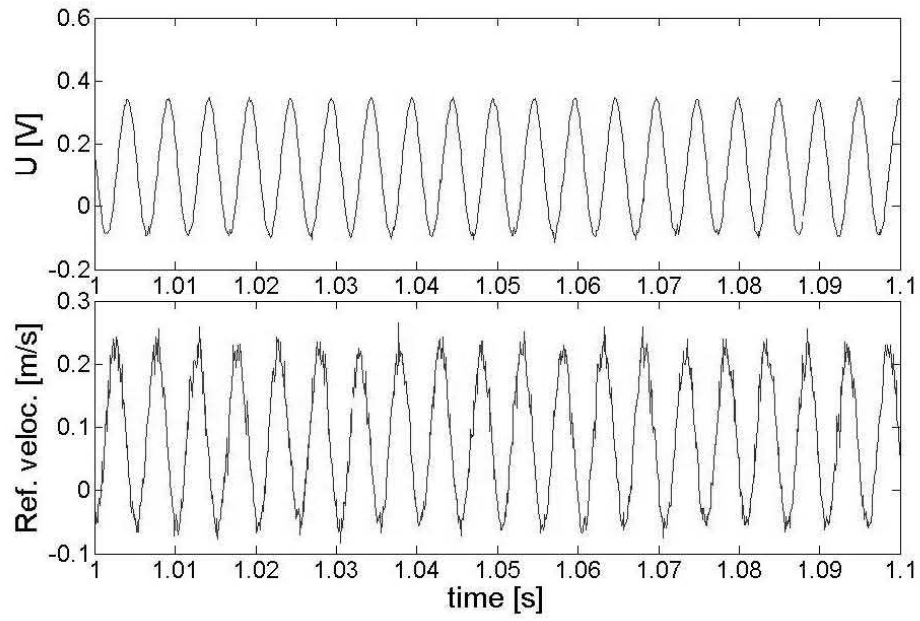
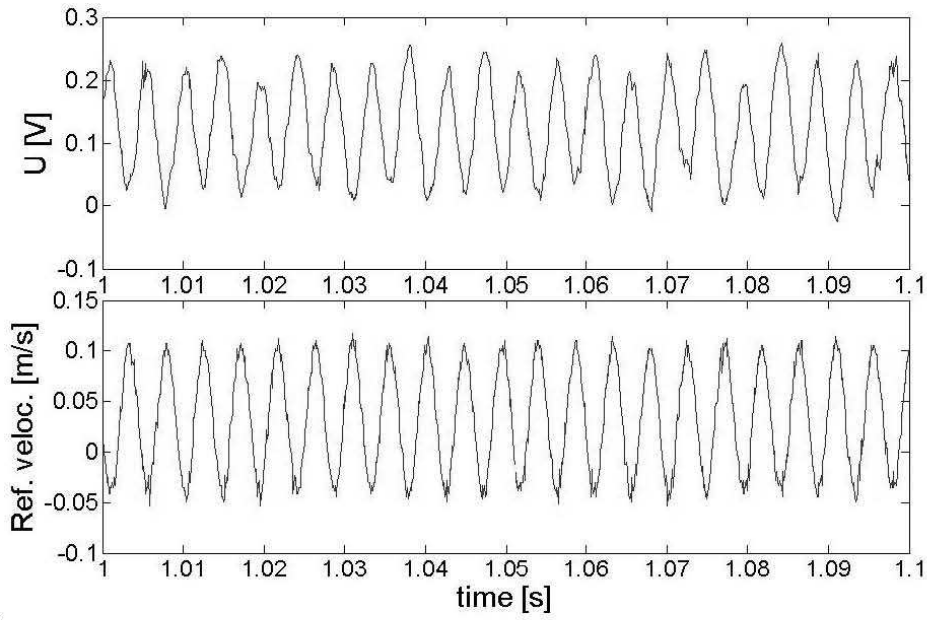


Figure 7. Time series for the second mode of the beam with fixed tip mass at the frequency $f = 76.25$ Hz (a) and moving mass at $f = 78.8$ Hz (b).



(a)



(b)

Figure 8. Time series for the third mode of the beam with fixed tip mass at the frequency $f = 197.19$ Hz (a) and moving mass at $f = 215.6$ Hz (b).

broadening visible for higher frequencies is caused by these nonlinearities. In Fig. 5 we compare the modal analysis results obtained for moving mass (violet line) and fixed mass (black line) for the first three modes which are the most important for energy harvesting. It is possible to notice that the spectrum is deformed by the extra degree of freedom of the moving mass and the nonlinear effects of friction and impacts including additional damping. The most visible effect is the shift of the mode III frequency to the higher frequency region. This could be a nonlinear effect of the stiffness changes with respect to the contact between the moving mass and beam. Simultaneously, this mode is characterized by a smaller velocity comparing to the case with the fixed mass. Comparing the peak values in the resonance we observe decreasing of the characteristic ranges velocities (Fig. 5) as the modes are not so pronounced in the case of the moving mass (see Fig. 3) where additional damping and nonlinear effects are present. On the other hand the first mode response is smeared in the system with moving mass.

Consequently, it is easy to notice the difference between the fixed and moving mass time series. The moving mass introduces the nonregular perturbation to both the output voltage and the moving frame displacement excited by a shaker (Figures 6 - 8). Clearly, it disturbs the voltage output signal, what is noticeable in the upper sides of 'b' parts of figures 6, 7, 8 for the first, second, and third mode, respectively. Interestingly, one can observe the nonlinear changes of the voltage output in the first mode even in the case with fixed mass (Fig. 6a). In spite of regularity, visible in the reference signal, the shape of $U(t)$ is of a non sinusoidal form. This may be due to the nonuniformity in beam mass distribution together with point mass attachment and nonvertical montage of the beam. Note that irregularities in the $U(t)$ have been also found in the higher modes. This was confirmed by Fourier transform. The moving mass causes changes in the various modes by different ways. In the first mode, the course of $U(t)$ is simply dominated by the moving mass disturbances. In the second mode, the time series of voltage output is deformed and modulated (Fig. 6a). Finally, in the third mode, the amplitude of voltage changes fairly random in the time domain.

In the Tab. 2 we present the standard deviation ratio: the voltage output to reference signal. This is smaller in all cases for the moving mass (the case with clearance). This is the effect of increasing damping in the system by enabling the mass to some relative motion.

4. Conclusions

We studied the effect of a moving mass in the simple beam system of energy harvesting. The modal analysis and time series responses confirms the the smearing of the resonance area, and consequently broadening the output voltage, around the mode I region. Nonlinear effects of the moving mass (contact loss, impact, friction) are presumably responsible to the

large frequency shift in the mod III area. These effects could improve the device efficiency.

However to tell more about that effect some more systematic studies are necessary for the fixed and moving mass configurations, including the frequency sweeps response of the voltage output.

Acknowledgments

This research was supported by the Polish National Science Center (A.R., M.B., and G.L.) under the grant agreement No. 2012/05/B/ST8/00080.

References

1. B. Nana, P. Woafu, *Physica A* 387, 3305 (2008).: Power delivered by an array of van der Pol oscillators coupled to a resonant cavity, *Physica A*, 378, 2008, 3305-3313.
2. S.M. Shahruz: Design of mechanical band-pass filters for energy scavenging, *J. Sound Vib.*, 292, 2006, 987998.
3. A. Erturk, J. M. Renno, and D.J. Inman: Modeling of Piezoelectric Energy Harvesting from an L-Shaped Beam-Mass Structure with an Application to UAVs, *J. Intell. Mater. Syst. Struct.*, 20, 2009, 529544.
4. G. Litak, M.I. Friswell, C.A.K. Kwiimy, S. Adhikari, M. Borowiec: Energy harvesting by two magnetopiezoelectric oscillators with mistuning, *Theor. App. Mech. Lett.*, 2, 2012, 043009.
5. K. Kucab, G. Gorski, J. Mizia: Energy harvesting in the nonlinear two-masses piezoelectric system driven by harmonic excitations, *Europ. Phys. J. Special Topics*, 222, 2013, 1607-1616.
6. S.P. Pellegrini, N. Tolu, M. Schenk, J.L. Herder.: Bistable vibration energy harvesters: A review, *Smart Mater. Struct.*, 22, 2012, 023001.
7. L. Gu, C. Livermore.: Impact-driven, frequency up-converting coupled vibration energy harvesting device for low frequency operation, *Smart Mater. Struct.*, 20, 2011, 045004.
8. C.P. Le, E. Halvorsen.: MEMS electrostatic energy harvesters with end-stop effects, *J. Micromech. Microeng.*, 22, 2012, 074006.
9. L. Gu and C. Livermore: Impact-driven, frequency up-converting coupled vibration energy harvesting device for low frequency operation, *Smart Mater. Struct.*, 20, 2011, 045004.
10. M.S.M. Soliman, E.M. Abdel-Rahman, E.F. El-Saadany, R.R. Mansour.: A wideband vibration-based energy harvester, *J. Micromech. Microeng.*, 18, 2008, 115021.

Andrzej Rysak, Ph.D.: Lublin University of Technology, Institute of Technological Systems of Information, Nadbystrzycka 36, PL-20-618, Poland, the author gave a presentation of this paper during one of the conference sessions (a.rysak@pollub.pl).

Michael Scheffler, Ph.D, D.Sc. Eng.: Technische Universität Dresden, Institut für Festkörpermechanik, Marschnerstrae 30 D-01307 Dresden, Germany (michael.scheffler@tu-dresden.de).

Joachim Gier, Ph.D. Eng.: Technische Universität Dresden, Institut für Festkörpermechanik, Marschnerstrae 30 D-01307 Dresden, Germany (joachim.gier@tu-dresden.de).

Marek Borowiec, Ph.D. Eng.: Lublin University of Technology, Department of Applied Mechanics, Nadbystrzycka 36, PL-20-618, Poland (m.borowiec@pollub.pl).

Grzegorz Litak, Professor: Lublin University of Technology, Department of Applied Mechanics, Nadbystrzycka 36, PL-20-618, Poland (g.litak@pollub.pl).